



HAL
open science

Thermoviscous acoustic propagation in thin rough tubes

Henri Boutin, Juliette Chabassier, Thomas H elie, Alexis Thibault

► **To cite this version:**

Henri Boutin, Juliette Chabassier, Thomas H elie, Alexis Thibault. Thermoviscous acoustic propagation in thin rough tubes. WAVES 2022 - 15th International Conference on Mathematical and Numerical Aspects of Wave Propagation, Jul 2022, Palaiseau, France. hal-03780126

HAL Id: hal-03780126

<https://hal.science/hal-03780126>

Submitted on 19 Sep 2022

HAL is a multi-disciplinary open access archive for the deposit and dissemination of scientific research documents, whether they are published or not. The documents may come from teaching and research institutions in France or abroad, or from public or private research centers.

L'archive ouverte pluridisciplinaire **HAL**, est destin ee au d ep ot et  a la diffusion de documents scientifiques de niveau recherche, publi es ou non,  emanant des  tablissements d'enseignement et de recherche fran ais ou  trangers, des laboratoires publics ou priv es.

Thermoviscous acoustic propagation in thin rough tubes

Henri Boutin¹, Juliette Chabassier², Thomas H elie¹, Alexis THIBAUT^{2,*}

¹S3AM team, STMS, 1 place Igor Stravinsky, 75004 Paris –France

²MAKUTU team, Inria Bordeaux Sud-Ouest, 200 avenue de la Vieille Tour, Talence – France

*Email: alexis.thibault@inria.fr

Abstract

Thermoviscous acoustic propagation in a tube with corrugated isothermal rigid walls is considered. At long wavelengths, it amounts to a 1D transmission line equation, in which the coefficients depend on the solution to a 2D diffusion problem. These coefficients are shown to display predictable behaviors at low, high, and intermediate frequencies. These results are demonstrated on a numerical example.

Keywords: roughness, thermoviscous acoustics, scale separation, losses

1 Introduction

Wind instruments made out of wood often exhibit small-scale detail (roughness) on the inner wall. It has been shown experimentally to modify the effective dissipation and dispersion of acoustic waves in the air inside the instrument [2]. However, this phenomenon is usually neglected in musical acoustics models.

This work proposes a computation method for thermoviscous acoustics in a thin tube with a rough (here, grooved) wall. It consists in separating the acoustic propagation, which occurs mostly in the longitudinal direction z (1D), from the viscous and thermal diffusion, which occurs mostly in the transverse directions (2D).

2 Long wavelength approximation

We consider a simplified rough tube, represented by a domain $\Omega = \Sigma \times \mathbb{R}$, where the cross-section $\Sigma \subset \mathbb{R}^2$ is the union of a disk of radius $R = 7.45$ mm, with smaller disks of radius $R_{\text{rough}} = 0.16$ mm intersecting its boundary, spaced by $w = 0.3$ mm (see Figure 1).

We assume that the acoustic velocity $\hat{\mathbf{u}}$, pressure \hat{p} , density and temperature are solutions to the time-harmonic linearized Navier-Stokes equations in Ω , with no-slip and isothermal boundary conditions. Assuming that the acoustic wavelength $\lambda = 2\pi c_0/\omega$ (where c_0 is the isentropic sound velocity, and parameter $\omega > 0$ is the an-

gular frequency) is much larger than both the tube radius R and the viscous and thermal characteristic lengths, then the pressure $\hat{p}(z)$ and total flow $\hat{U}(z) = \iint_{\Sigma} \hat{\mathbf{u}}(x, y, z) \cdot \mathbf{e}_z dx dy$ are solution to a 1D transmission line equation [3]

$$\begin{cases} \frac{d}{dz} \hat{p}(z) + Z_v \hat{U}(z) = 0, \\ \frac{d}{dz} \hat{U}(z) + Y_t \hat{p}(z) = 0. \end{cases} \quad (1)$$

with $Z_v = \frac{1}{1-K_v} \frac{i\omega\rho_0}{|\Sigma|}$, $Y_t = (1 + (\gamma - 1) K_t) \frac{i\omega|\Sigma|}{\rho_0 c_0^2}$, where ρ_0 is the static density, $|\Sigma|$ is the cross-section area, and the coefficients $K_v = 1 - \langle \psi_{\beta_v} \rangle$, $K_t = 1 - \langle \psi_{\beta_t} \rangle$, quantify the influence of the viscous and thermal effects respectively, and would be zero in the lossless case. Constants $\beta_v = \mu/\rho_0$ and $\beta_t = \kappa/\rho_0 C_p$ are related to the viscous and thermal diffusion rates, and $\langle \psi_{\beta} \rangle$ is the mean over Σ of the solution ψ_{β} to a heat equation on the cross-section

$$\begin{cases} i\omega \psi_{\beta}(x, y) - \beta \Delta \psi_{\beta}(x, y) = i\omega & \text{on } \Sigma \\ \psi_{\beta}(x, y) = 0 & \text{on } \partial\Sigma. \end{cases} \quad (2)$$

We propose to solve the equations sequentially, by first calculating the solutions ψ_{β_v} and ψ_{β_t} of the transverse problem (§3-4), and then by using the resulting values of K_v and K_t to solve the transmission line equation (§5).

3 Analysis in the harmonic domain at low, high and medium frequency

Since the solution ψ_{β} of the transverse problem depends on the frequency, so do K_v and K_t . Since K_v and K_t are equal up to a frequency scaling factor of $\beta_v/\beta_t = \mu C_p/\kappa = 0.71$ for air, only K_v is considered hereafter.

In the low frequency limit, ψ_{β} tends to zero and therefore $\lim_{\omega \rightarrow 0} K_v = 1$. In the high frequency limit, boundary layers form in the vicinity of the walls, with thickness $\delta = \sqrt{\beta/\omega}$, and ψ_{β} quickly approaches 1 away from the boundaries [1]. One can show that the influence of the boundary layers is asymptotically

$$K_v(\omega) = (1 - i) \frac{|\partial\Sigma|}{|\Sigma|} \sqrt{\frac{\beta_v}{2\omega}} + o(\omega^{-1/2}). \quad (\text{HF rough})$$

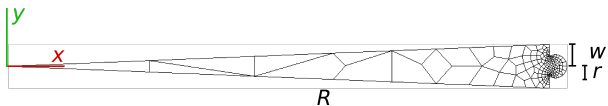


Figure 1: Mesh of the "slice" of Σ used for the 2D simulation

This suggests that increasing the perimeter-to-area ratio $|\partial\Sigma|/|\Sigma|$ should increase the amount of losses. Moreover, in the high-frequency limit, thermal and viscous effects contribute equally to dispersion (real part) and dissipation (imaginary part).

As the frequency decreases, the boundary layer thickness may exceed the characteristic size R_{rough} of the asperities. We would thus expect K_v to follow approximately equation (HF rough), but with a frequency-dependent effective perimeter length. If $R_{\text{rough}} \ll R$, a regime should appear where Σ can be approximated as a disk:

$$K_v(\omega) \approx (1 - i) \frac{2}{R} \sqrt{\frac{\beta_v}{2\omega}}. \quad (\text{HF smooth})$$

4 Numerical calculations: 2D problem

Equation (2) is solved on a 2D mesh representing a small triangular portion of domain Σ . The domain is virtually symmetrized by using Neumann conditions on the cutting lines. Calculations are performed using high-order finite element library Montjoie. Elements of order 8 are used, leading to a relative L^2 error lower than 2×10^{-4} at all frequencies.

The solution ψ_{β_v} is computed at 30 frequencies with geometric progression spanning 6×10^{-4} Hz to 20 kHz. The dependency of K_v with respect to frequency is plotted in figure 2, together with the asymptotes predicted by equation (HF rough) for a smooth tube and for the considered rough tube.

The three regimes predicted in the previous section are visible: the low-frequency asymptote below 10^{-2} Hz (below human hearing, 20 Hz–20 kHz), the high-frequency asymptote (HF rough) above 1 kHz, and a region from 10^{-1} Hz to 10^1 Hz where K_v is close to the "smooth tube of same radius" approximation (HF smooth).

5 Solving the transmission line equations

System (1) is solved for the values of $K_v(\omega)$ and $K_t(\omega)$ computed in §4, using high-order 1D finite elements [4]. Assuming that the tube is closed with condition $\hat{U}(L) = 0$ at $L = 238.5$ mm, and driven with unit flow $\hat{U}(0) = 1$, we compute

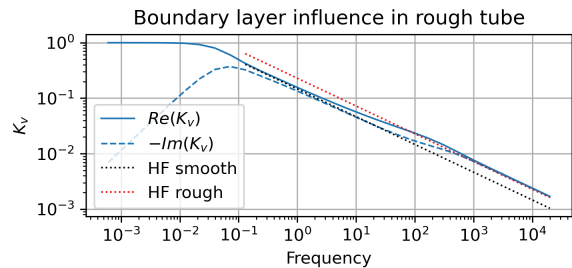


Figure 2: Real and imaginary parts of loss coefficient K_v in the rough tube, as a function of frequency.

the acoustic impedance $Z = \hat{p}(0)/\hat{U}(0)$. The result is plotted in figure 3 for the rough tube and for a smooth circular tube of same radius.

We observe a resonance around 1430 Hz, which remain of finite amplitude because of the dissipation. The roughness appears to lower the quality factor of the resonance, and to shift the resonance frequency down by about 3Hz.

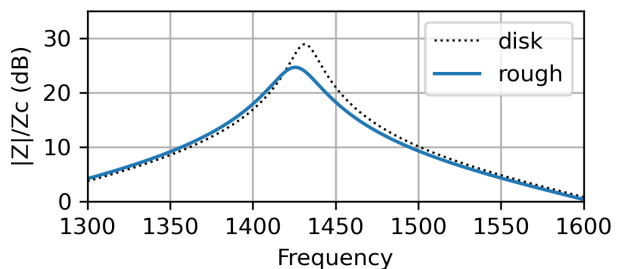


Figure 3: Calculated acoustic impedance on tubes without/with roughness.

6 Perspectives

A first perspective is to extend the results from the time-harmonic domain to the Laplace and the time domain, in view of using the theory of diffusive representations to provide time-domain simulations of rough tubes. A second perspective is to consider the case of tapered tubes, which encompass more musical instruments.

References

- [1] M. Berggren, A. Bernland, and D. Noreland, *Journal of Computational Physics*, 371:633–650, 2018.
- [2] H. Boutin et al. 14^{ème} Congrès Français d'Acoustique (CFA'18), pages 685–691, Le Havre, 2018.
- [3] M. R Stinson. *Journal of the Acoustical Society of America*, 89(2):550–558, 1991.
- [4] R. Tournemene and J. Chabassier. *Acta Acustica united with Acustica*, 105(5):838–849, 2019.